Optimal PV array configurations for partial shading conditions

Parween R. Kareem[1], Sameer Algburi[2], Husniyah Jasim[1], Fattah H. Hasan[1]
[1]Department of Electrical Technique, Al-Hawija Technical Institute, Northern Technical University, Kirkuk, Iraq
[2]College of Technical Engineer, Al-Kitab University, Kirkuk, Iraq

Article Info

Article history:

Received Mar 16, 2023
Revised Jun 7, 2023
Accepted Jun 17, 2023

Keywords:

Fill factor
Global maximum power point
mismatch losses
Partial shading
PV array configurations

ABSTRACT

Increasing the effectiveness of photovoltaic (PV) power generation systems is a major barrier to their widespread use. Partial shading conditions (PSCs), which are caused by nearby objects like trees, buildings, and clouds, reduce the energy produced by PV systems and may be mitigated by the reconfiguration of PV arrays. A novel approach dubbed a modified series-parallel (MSP) setup, was suggested in this paper and compares its performance to four PV configuration strategies: series-parallel (SP), total-cross-tied (TCT), bridge-linked (BL), and honey-comb (HC). A 3×3 solar array is used in five partial shading arrangements. MATLAB/Simulink simulates all shading conditions. This study indicated that MSP delivers high performance and is superior to all other configurations in terms of maximum power in even and uneven row-shaded cases. in the case of an even column shaded, the performance of (SP, BL, HC, and TCT) was equal in terms of the maximum power obtained, while MSP was the least in comparison. the performance of the TCT configuration was the best compared to the other configuration when shading the PV system vertically unevenly. Finally, for diagonal shading, TCT and MSP configurations work best. Shading loss, mismatch loss and fill factor (FF) results were also compared.

Corresponding Author:

Parween R. Kareem
Department of Electrical Techniques, Al-Hawija Technical Institute, Northern Technical University
Al-Zawra Neighbourhood, Kirkuk, Iraq
Email: preween_hwj@ntu.edu.iq

1. INTRODUCTION

The majority of the world's energy consumption still comes from conventional, nonrenewable sources, which have contributed to hazardous emissions that have accelerated global warming and had other severe adverse effects on the environment and climate [1]–[4], Since the launch of the Earth Summit (Rio de Janeiro) in 1992 and the summits that followed, international organizations have called for the necessity for governments to implement their promises to achieve fair and sustainable development; this is because energy is the basis for all sectors of the economy and human life [5]. It has become necessary to start searching for alternative renewable energy sources to preserve the environment, ensure its sustainability, and meet the increasing demand for energy as a result of the increasing population density [2], [6]. The widespread availability of solar irradiation, the ease of rooftop installation, and photovoltaic (PV) technology's low environmental impact have contributed to its rising popularity in recent years [5], [7]–[9]. The process of generating energy by converting solar photons through semiconductors such as silicon is known as the PV effect, and this is the basis for the work of solar panels [7]. The most important factors affecting PV systems' performance and reducing efficiency are temperature, solar power, and partial shading [8]–[10]. Partial shading is one of the main problems and obstacles that limit the maximum utilization of the PV energy system, as it is a very influential factor in the productivity of solar panels unless taken into account, some types of shade from objects such as dirt, bird droppings and tree leaves can be treated with regular cleaning of the panels and should others are taken into account in the design and calculations [11]–[13].

PV system consists of a group of solar panels, which in turn consists of many solar PV cells, suppose the shadow falls even on only one part of the solar panels in an array. In that case, the output of the entire system may be at risk, which may lead to overheating and damage to the solar panels, and from here comes the importance of the diode, which prevents the flow of electric current in the opposite direction and thus protects the solar panel from hot spots [13]. These diodes give the PV array's I-V curve several steps and its P-V curve multiple peaks [14]. The p-V curve has several peaks, one of them represents the global maximum power point (GMPP), while the other peaks are local maximum power points (LMPPs) [9], [15], [16]. Besides the by-pass diode, reconfiguring a PV array is a low-cost way to increase a PV array's maximum achievable power in PSCs. Installing semiconductor switches and power electronic converters doesn't cost any more with this method [17], [18]. Some researchers have tried the following methods to maximize power by using reconfiguration techniques. Bingöl and Özkaya [8] use 6×6 PV arrays in five configuration schemes: series S, Series-parallel (SP), bridge-link (BL), total-cross-tied (TCT), honeycomb (HC) under six PSCs. TCT design outperforms other arrangements in maximum power under all partial shading conditions. Pendem and Mikkili [13] simulated the performance of Series (S), SP, BL, and HC PV array designs under several PS patterns, including uneven rows, uneven columns, diagonal, random, short and narrow rows, short and wide, long and narrow, and long and wide shading patterns, HC design performs better in MATLAB/Simulink simulations of 5×5 PV array systems under varying shading patterns, making it a viable option for central inverter grid-connected and freestanding PV systems.

Pareek and Dahiya [15] simulated SP, TCT, and BL connectivity systems in MATLAB/Simulink. According to several case studies, the SP configuration generates more power and current than the TCT configuration when the tangent is expected to travel from left to right along the bottom row of modules, and TCT interconnection generates more power and current than SP when the tangent is expected to move up the leftmost column of modules from bottom to top. Khaleel and Mahmood [17] propose a novel shadow dispersion approach (NSDS) to reduce partial shading and enhance output power in solar PV arrays. The proposed shadow dispersion strategy was employed on a 6×3 solar array to tackle the partial shade issue that du Ku and gradient left unsolved. Power generation increased by almost 30%.

Patel and Agarwal [19] presented and constructed a MATLAB-based simulator and learning tool for modelling S and SP configurations to calculate maximum power, predict PSCs, and predict nonlinear I-V and P-V characteristics. The data show that array layout and shading pattern affect GMPP size, solar irradiation, and temperature. Belhachat and Larbes [20] tested PV array topologies with uniform and unequal row and column shading patterns. Despite its redundancy, the TCT configuration performs better in simulations. Elyaqouti *et al.* [21] examined several solar array layouts' energy performance and electrical behaviour under PSCs to discover the best and most cost-effective one. S, parallel (P), SP, TCT, BL, and HC were examined. The simulation showed how PV arrays transform solar energy into useful power under uniform and partial shadow settings. Sajwan *et al.* [22] compare rearrange square (RS) against TCT, HC, BL, and SP based on three performance indices: GMPP, power loss, and F.F. Physical relocation-based setup RS increase power generation under diverse shadow conditions. Picault *et al.* [23] changed PV array module connections to reduce partial shade mismatch losses. Jaén University measured a 2.2 kW plant.SP, TCT, and BL connectivity schemes provide outcomes. TCT architecture reduces mismatch losses during PV array shading without decreasing plant efficiency.

Madhusudanan *et al.* [24] investigate the potential of Magic Su-Do-Ku-based static reconfiguration for increasing the output of a PV array under partially shaded situations. The previously described static reconfiguration solutions achieve the power increase due to inefficient shadow dispersion. The TCT connections are not modified in this suggested Magic Su-Do-Ku-based interconnection structure, but the goal of uniform shadow dispersion is still achieved. Several shading patterns and their effects on the PV array's maximum power point (MPP) have been investigated to determine the optimal shading conditions for optimum power production. The efficiency of the proposed layout is shown by the positive outcomes obtained with different types of shading. Krishna and Moger [25] This research presents an improved Su-Do-Ku reconfiguration pattern for a 9×9 TCT PV array to maximize power production under partial shadowing. This method arranges TCT array PV modules in the Su-Do-Ku pattern without changing electrical connections. The GMPP, mismatch losses, fill factor (FF), and efficiency of the proposed pattern are compared to current PV array designs. This article concludes that the new Su-Do-Ku PV array configuration increases global maximum power under all shading circumstances.

In this study, a new method was proposed for connecting solar panels in a PV array to increase the efficacy of the photovoltaic system. This method is a modification of the SP method and is referred to as the MSP configuration. It is evident from the obtained results that it outperforms the other configurations examined in this research for certain partial shading types in terms of (maximum power obtained, mismatch loss and FF).

2. MODELING OF PV MODULE

A variety of PV cell modelling methodologies, including single-, double-, and triple-diode models, have already been given by several researchers [19]. In Figure 1, a single-diode PV cell model has been chosen for easier comprehension. The current generated from the single PV cell is [23]:

$$I = I_L - I_O\left(e^{q(V+IR_S)/n_S AKT} - 1\right) - \frac{V+IR_S}{R_P} \quad (1)$$

where (I_L) photo-generated current, (I_O) is the saturation current, (R_S) is series resistance, (R_P) is shunt resistance, (K) is boltzmann's constant, $(q)$is electron charge, (n_s) is the number of cells connected in series and (T) is the cell temperature (kelvin).

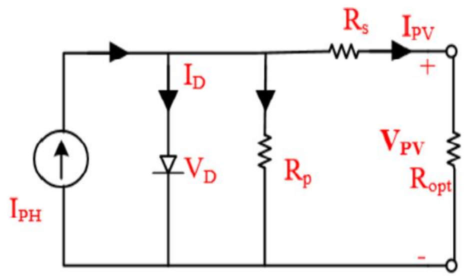

Figure 1. Single-diode circuit model of PV cell [26]

The study details the system's PV module properties, shown in Table 1. The I-V (current-voltage) and P-V (power-voltage) characteristics of the PV module used in the system are also shown in Figure 2. The graphical depiction in Figure 2(a) makes it abundantly evident that the quantity of solar radiation incident on the solar panel directly affects how much current it produces. Thus, as shown in Figure 2(b), the electricity generated by the solar panel rises when solar radiation increases and vice versa. These findings highlight the connection between solar radiation, current, and the PV module's power production.

Table 1. PV module parameter used in the system at STC (1,000 W/m^2 and 25 ^{o}C)

Parameter	Variable	Value
Maximum power point voltage	V_{mpp}	10.32
Maximum power point current	I_{mpp}	8.07
Maximum power	P_{mpp}	3.28
Open circuit voltage	V_{OC}	12.64
Short circuit current	I_{sc}	8.62
Fill factor	FF	76%
Number of series cell	N_S	20
Temperature coefficient of Isc	Isc T	0.063701
Temperature coefficient of $V_{O.C}$	Voc T	-0.33969

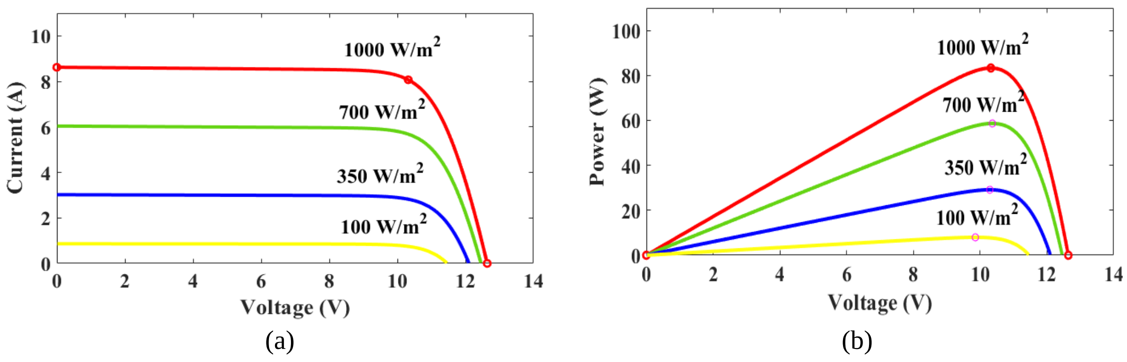

Figure 2. PV module characteristics for different solar irradiance (a) I-V characteristics and (b) P-V characteristics

3. PV ARRAY CONFIGURATIONS

Solar energy systems are designed either to be independent of the electrical network by a few kilowatts (which is used in villages, rural areas and remote areas that are not connected to the national electrical network) or to be connected to the electrical network to supply it with several megawatts [17]. Solar panels are assembled and connected to form a PV array to suit the voltage and current of the electrical network or the requirements of the loads, and this is done in several ways; Figure 3 is a diagrammatic representation of the many configurations of PV arrays [8], [18]. Within the scope of this article, five distinct array configurations will be discussed. They include SP, TCT, BL, HC, and MSP.

Figure 3(a) presents an illustration of the SP arrangement. To achieve the required output voltage, it is necessary to first link all of the modules in the form of a series connection and then join these series connections in parallel [18], [23]. Figure 3(b) illustrates the TCT arrangement. The SP configuration is produced by attaching crossties across each module row. Each row’s voltage and column’s current are identical in this configuration [22]. The BL setup may be shown in Figure 3(c). There is a bridging unit that has four separate modules. The parallel connection of those same modules follows the series connection of two modules in a bridge. Cross ties are used to connect the bridges in a network [8], [19], [22], [27]. Figure 3(d) illustrates the HC arrangement. The HC configuration is a tweaked variant of the BL design, and the size of its bridge may be adjusted [19], [22], [27]. The novel approach suggested as a result of this study is denoted by the abbreviation MSP and can be seen in Figure 3(e). This method involves first connecting the solar panels in parallel in the form of three groups, which are then linked in series.

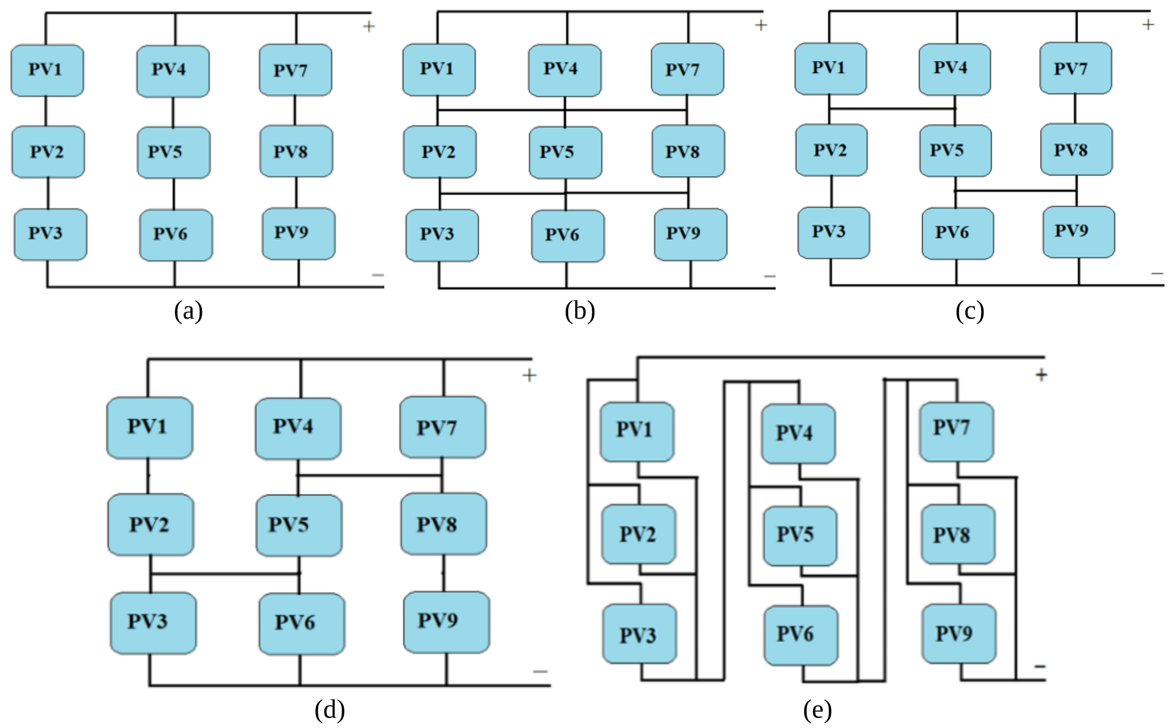

Figure 3. PV Module interconnection styles; (a) SP, (b) TCT, (c) BL, (d) HC, and (e) MSP interconnections

4. EFFECT OF ALTERNATIVE ARRAY CONFIGURATION IN NORMAL OPERATING CONDITIONS

First, it is necessary to determine whether BL, HC, TCT, and SP configurations do not reduce power generation under normal conditions (N.C) compared to the conventional interconnect SP configuration, that is, without shade, PV characteristics of all possible PV array designs measured under the same conditions (1,000 W/m^2 and 25 ^{o}C) are shown in Figure 4, where Figure 4(a) and Figure 4(b) represent I-V and P-V curve respectively. The maximum power that a 3×3 PV array may generate is outlined in Table 2, which can be found in Table 2. According to the findings, each of the five array architectures has a single power peak and comparable values for their maximum power point.

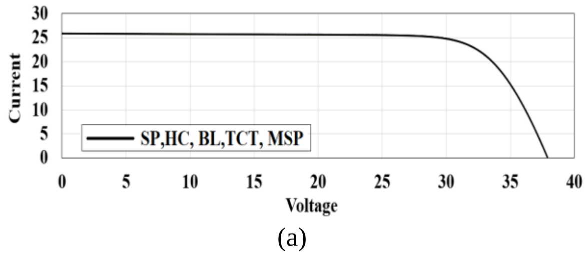

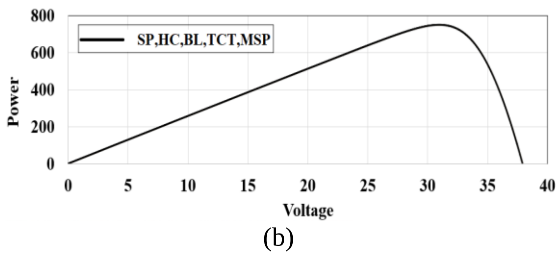

Figure 4. Characteristic of PV array configuration at the uniform condition (a) I-V characteristic and (b) P-V characteristic

Table 2. Under uniform irradiance conditions

Configuration	Vo.c (V)	Isc (A)	P_{max} (w)	V_{max} (V)	I_{max} (A)	FF (%)
SP	37.89	25.86	749.506	30.968	24.203	0.7649
TCT	37.89	25.86	749.508	30.943	24.222	0.7649
BL	37.89	25.86	749.508	30.942	24.222	0.7649
HC	37.89	25.86	749.507	30.955	24.212	0.7649
MSP	37.89	25.86	749.507	30.955	24.213	0.7649

5. RESULTS AND DISCUSSION

This research aims to present the simulation results of the five possible configurations for PV arrays under different PSCs to determine the optimal configuration. The performance of the different PV configurations was compared in terms of maximum power, mismatching losses, shading losses and FF during different partial shading cases which are simulated in MATLAB/Simulink. Shading loss is the array's maximum power without shading minus the modules' maximum power in a partial shade. At the same time, mismatch loss is the difference between each module's maximum power and the global maximum power point. FF is the ratio of maximum global power to the product of the array configuration's open circuit voltage and short circuit current under the PSCs. When FF approaches unity, system performance improves. To explore the effectiveness of various designs of PV arrays, the experiments were carried out on a 3×3 PV array while operating under PSCs. The partial shading cases considered for this research are shown in Figure (5):

- Case 1. Even row shading, in which the solar irradiance (G) value of the first row is 700 W/m2 for the whole panel and the (G) value of the remaining columns is 1,000 W/m2. This case shwon in Figure 5(a).
- Case 2. Uneven row shading in which the (G) value of the first row is 100 W/m2, 350 W/m2,700 W/m2 respectively, and other rows are 1,000 W/m2. This case shwon in Figure 5(b).
- Case 3. Even column shading, in which the (G) value of the first column is 700 W/m2 for the whole panel and the (G) value of the remaining columns is 1,000 W/m2. This case shwon in Figure 5(c).
- Case 4. Uneven column shading, with the (G) value of the first column coming in at 100 W/m2, 350 W/m2, and 700 W/m2 accordingly, whereas the value of the remaining column is 1,000 W/m2. This case shwon in Figure 5(d).
- Case 5. The G value of the array's diagonal is 700 W/m2, whereas the G value of the other modules is 1,000 W/m2. This case shwon in Figure 5(e).

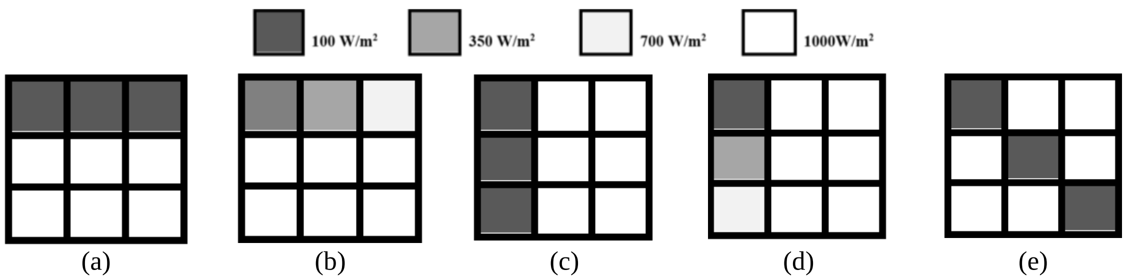

Figure 5. Partial shading (a) Case 1, (b) Case 2, (c) Case 3, (d) Case 4, and (e) Case 5

The simulation results of PV array configurations under shading cases are represented in Table 3. For case 1, as shown in Figure 6. MSP configuration presents the best performance with the highest maximum power 675.55 W at 30.99328 V and 21.79673 A, and also represents no LMPP, while the other configurations SP, TCT, BL and HC provide the same maximum power which is in the order of 574.76 W and represent one LMPP. As for FF as shown in Figure 7, SP, TCT, BL, and HC have the same value which is 0.58, while its value for the MSP is 0.76. Figure 8 show the mismatch losses; the MSP configuration presents the lowest value 0.0178 W as compared with the other configuration where the mismatch losses value them are 100.743 W. For all configurations, shading loss values give the same value in this case. The findings shown in this scenario, which include the maximum power obtained, FF, partial shading, and mismatch losses, clearly demonstrate the MSP configuration's superiority over the other configurations.

Table 3. Simulation results of shading cases

		Global peak parameter							
Cases	Configuration	Vo.c (V)	Isc (A)	P_{max} (w)	V_{max} (V)	I_{max} (A)	FF (%)	Shading losses	Mismatch losses
Case 1: even row shaded	SP	37.7304	25.8899	574.76	32.72496	17.56362	0.588398253	73.936	100.8012
	TCT	37.92	25.8899	574.76	32.72496	17.5636	0.585455595	73.936	100.8008
	BL	37.92	25.8899	574.76	32.7376	17.55681	0.585455305	73.936	100.802
	HC	37.92	25.8899	574.76	32.725	17.5654	0.585516311	73.936	100.743
	MSP	37.92	23.30149	675.55	30.99328	21.79673	0.764551708	73.936	0.0178
Case 2: uneven row shaded	SP	37.92	25.8899	482.626	19.9712	24.1661	0.491600174	152.221	114.659
	TCT	37.92	25.8899	482.626	19.9712	24.1661	0.491600174	152.221	114.659
	BL	37.92	25.8899	482.626	19.9712	24.1661	0.491600174	152.221	114.659
	HC	37.92	25.8899	482.626	19.9712	24.1661	0.491600174	152.221	114.659
	MSP	37.92	23.2989	558.027	31.8781	17.505	0.631612618	152.221	39.258
Case 3: even column shaded	SP	37.92	23.3015	675.552	30.9933	21.7967	0.764550821	73.936	0.018
	TCT	37.68	23.28	675.552	31.00592	21.78781	0.770130514	73.936	0.018
	BL	37.743	23.3015	675.552	30.9933	21.7967	0.768136267	73.936	0.018
	HC	37.92	23.3015	675.552	30.9933	21.7967	0.764550821	73.936	0.018
	MSP	37.92	25.8899	574.769	32.725	17.5636	0.58545631	73.936	100.801
Case 4: uneven column shaded	SP	37.4902	23.3006	526.16	31.0438	16.9489	0.602325892	152.221	71.125
	TCT	37.5	23.23	558.03	31.86544	17.51208	0.640363669	152.221	39.255
	BL	23.2996	37.5029	536.402	31.4989	17.0293	0.613873473	152.221	60.883
	HC	37.92	23.2996	536.4	31.4989	17.0292	0.607117624	152.221	60.885
	MSP	37.92	25.8899	482.626	19.9712	24.1661	0.491600174	152.221	114.659
Case 5: diagonal shaded	SP	37.92	25.8899	574.77	32.72496	17.56371	0.585459261	73.936	100.7983
	TCT	37.92	23.30149	675.55	30.99328	21.79678	0.764553462	73.936	0.0163
	BL	37.7304	25.8899	574.77	32.7376	17.55685	0.588398632	73.936	100.8009
	HC	37.92	25.8899	574.77	32.7376	17.5569	0.585458306	73.936	100.8
	MSP	37.92	23.30149	675.55	30.99328	21.79673	0.764551708	73.936	0.0178

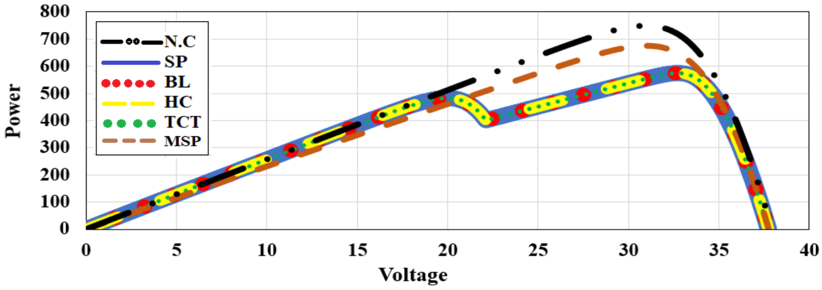

Figure 6. Even row shaded

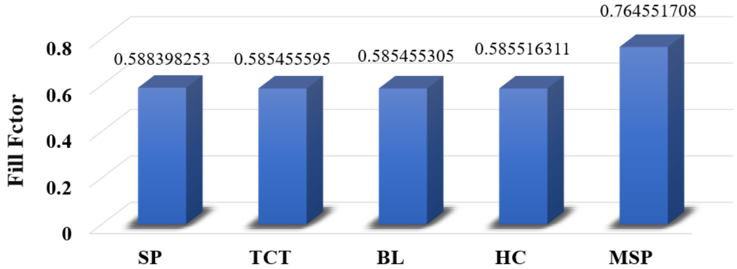

Figure 7. Fill factor of PV array configurations in even row shaded

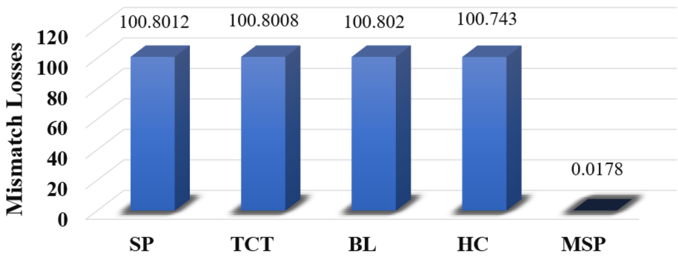

Figure 8. Mismatch losses of PV array configurations in even row shaded

For case 2, as shown in Figure 9, the MSP configuration presents the best performance with the highest maximum power or the GMPP at 558.027 W at 31.8781 V and 17.505 A, and this configuration represents the only two LMPPs at 394 W and 194 W respectively, as for the other configurations SP, TCT, BL, and HC, P-V curves coincide with each other and the maximum power is achieved as it reaches the value of 482.626 W. SP, TCT, BL, and HC has the same FF value which is 0.491, while its value for the MSP is 0.631, as for mismatch losses; the MSP presents the lowest value 39.258 W as compared with the other configuration where the mismatch losses value for them is 114.659 W, the results of the FF and mismatch losses are shown in the Figures 10 and 11. For all configurations, partial shading loss values give the same value which is 152.221 W. The results presented in this case show a clear superiority of the MSP configuration through the maximum power obtained, the FF, partial shading, and mismatch losses.

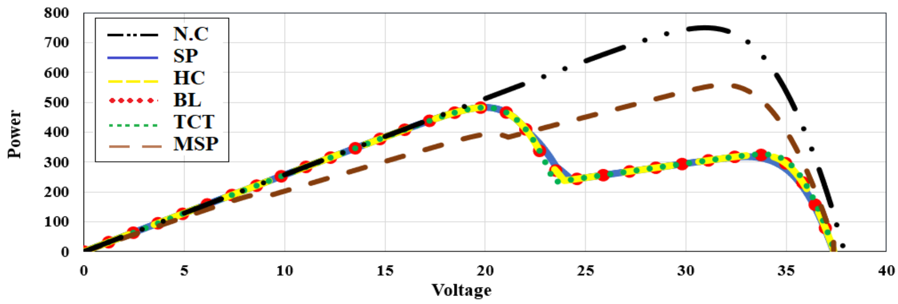

Figure 9. Un even row shaded

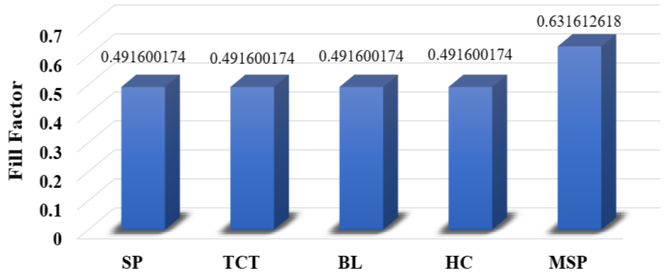

Figure 10. Fill factor PV array configurations of un even row shaded

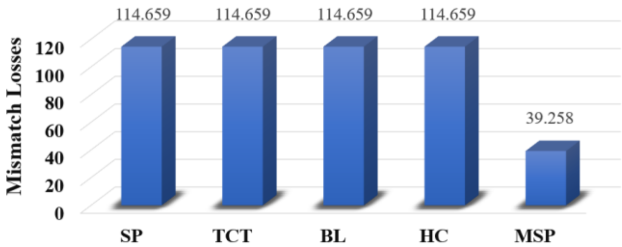

Figure 11. Mismatch losses of PV array configurations of un even row shaded

In case 3, as shown in Figure 12. Where the shadow falls on the panels located in the first column equally and obscures the light falling on them by 30%, the best performance is for SP, BL, HC, and TCT configuration, where the GMPP is achieved by 675.55 W; no local peaks LMPP appeared in P-V curve. MSP configuration generates the least maximum power of 574.7 W at 32.725 V and 17.563 A by representing only one LMPP at 482 W. FF for SP, BL, HC, and TCT configuration is equal to (0.764550821, 0.768136267, 0.764550821, 0.770130514) respectively, it is more than the FF of the MSP which is equal to (0.58545631), this is illustrated in the Figure 13. As for mismatch losses as shown in Figure 14, the SP, BL, HC and TCT configurations are present 0.018 W, while the mismatch losses for MSP are 100.801 W. For all configurations, partial shading loss values give the same value which is 73.936 W. It is noted from the aforementioned that the PV system’s best performance in this case study is achieved in SP, BL, HC, and TCT configurations.

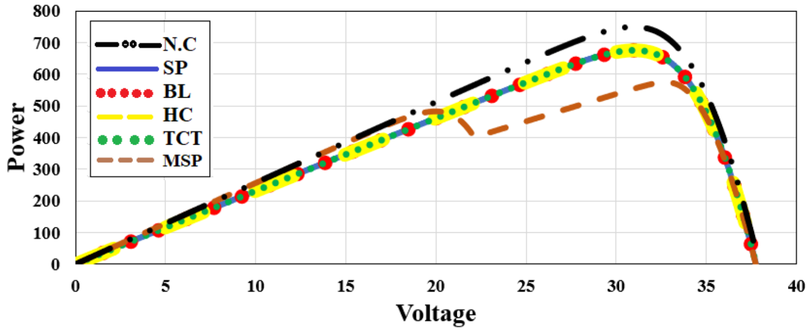

Figure 12. Even column shaded

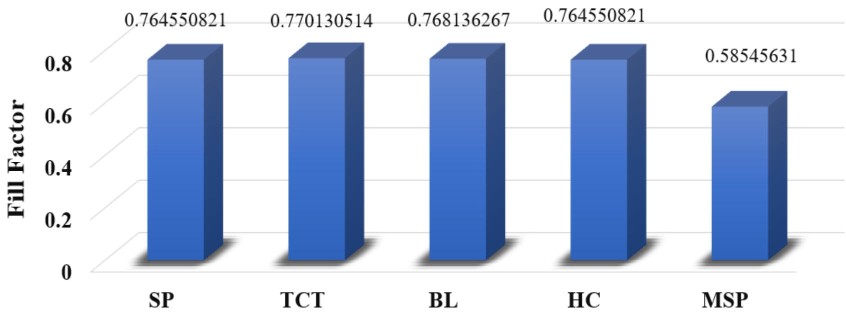

Figure 13. Fill factor of PV array configurations of even column shaded

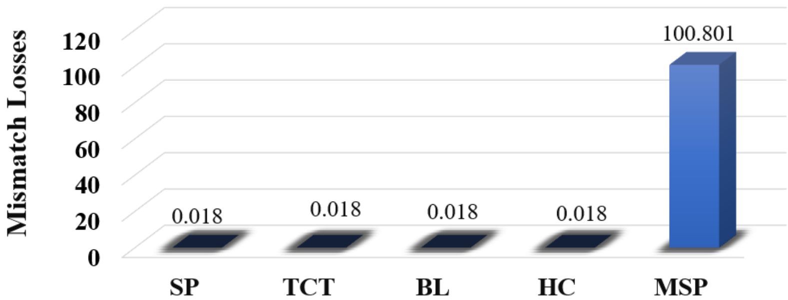

Figure 14. Mismatch losses of PV array configurations of even column shaded

In case 4, it is noted in Figure 15, the best performance in terms of maximum power, FF and mismatch losses is for TCT configuration, where its value 558.03 W, 0.64 and 39.255 W respectively, there are two LMPPs in P-V curve at 394 W and 194 W, as for the P-V curves for the HC and BL configurations, they match so that they achieve the same value for each of the maximum power, FF, and mismatch losses, as their value is (536 W, 0.61, 60.88 W) respectively; there are two LMPPs in P-V curve at 421 W and 200 W. There is a slight difference in the performance of the system in the SP configuration; the maximum power is 526 W, while the FF and the mismatch losses are 0.6, 71.125 W, respectively, and tow LMPP at 434 W and 212 W. The performance of the MSP configuration is the least efficient method in this case study, the global maximum power GMPP is 482.6 W by representing only one LMPP at 324 W, and the FF and the mismatch losses are (0.49, 114.659 W), respectively. Figures 16 and 17 show the results of the FF and mismatch losses. Patrial shading loss values give 152.221 W for all configurations.

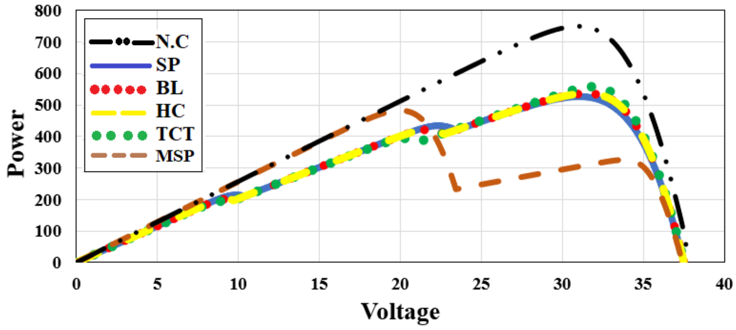

Figure 15. Un even column shaded

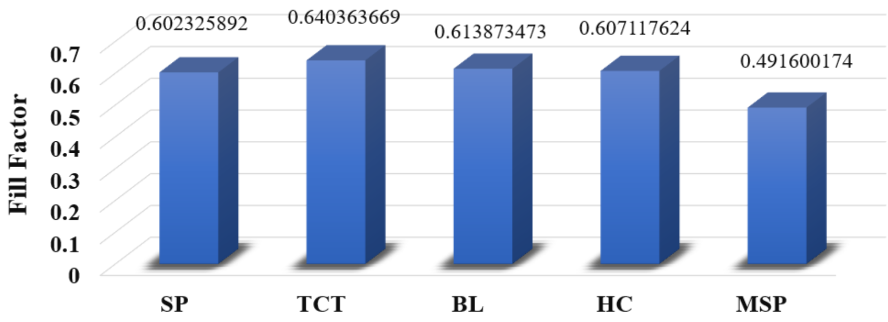

Figure 16. Fill factor of PV array configurations of un even column shaded

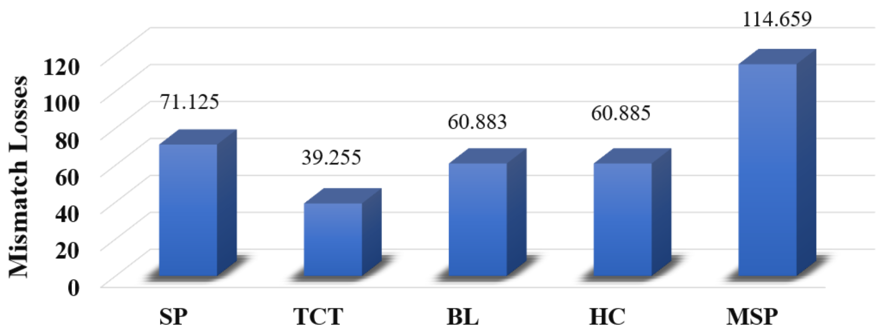

Figure 17. Mismatch losses of PV array configurations of un even column shaded

For case 5, as shown in Figure 18, the P-V curve for TCT and MSP coincides, they present the best performance where the GMPP is 675.55 W at 30.99328 V and 21.79673 A with no LMPP. As for SP, BL and HC configurations, the power curves for them coincide and the GMPP is 574.77 W with one LMPP at 483 W, they have the same FF value which is very close, ranging around (0.585), while the FF for the TCT and the MSP configurations are (0.76). As for mismatch losses; the TCT configuration presents the lowest value 0.0163 W, while the mismatch losses for the MSP are 0.0178 W. for the other configurations, the mismatch losses value them are 100.8 W. The results of the fill factor and mismatch losses are shown in Figures 19 and 20. For all configurations, shading loss values give the same value in this case which is 73.936 W.

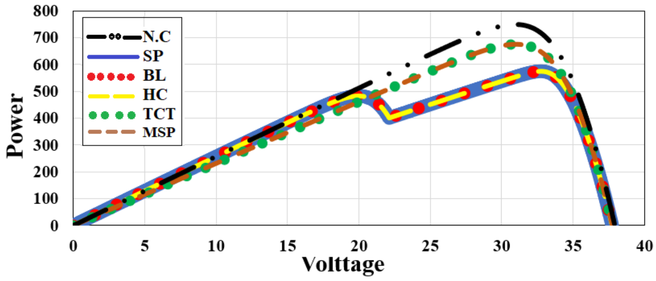

Figure 18. Diagonal shaded

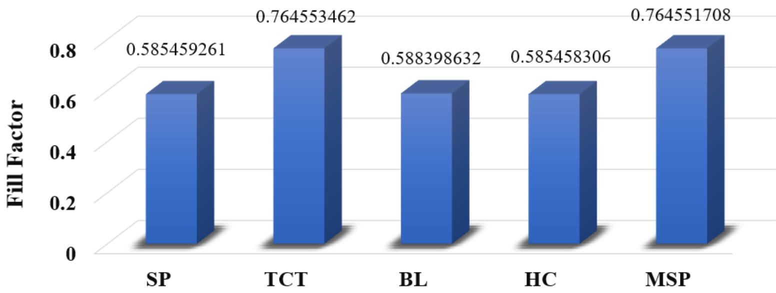

Figure 19. Fill factor of PV array configurations of diagonal shaded

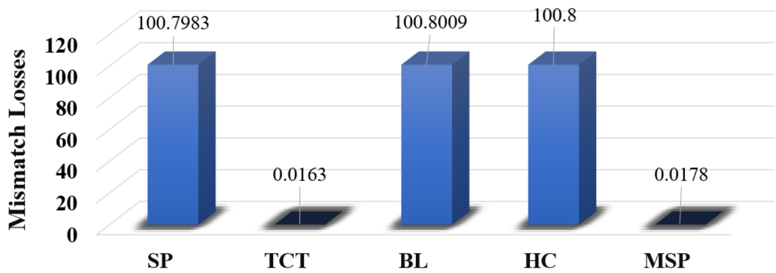

Figure 20. Mismatch losses of PV array configurations of diagonal shaded

6. CONCLUSION

In this research, a novel PV configuration termed MSP was proposed. A thorough comparative analysis was conducted taking into account the SP, TCT, BL, HC, and MSP PV array designs and five different partial shading scenarios. This was accomplished by doing MATLAB/Simulink simulations of all possible setups for various shading scenarios on a 3×3 PV array. All possible PV array configurations provide the same maximum power under N.C. Nevertheless, the efficiency of various PV array configurations varies depending on the degree of shading present. For case 1, the MSP configuration produces the maximum power 675.55 W, whereas the SP, HC, BL, and TCTS configurations all provide the same amount of maximum power 574.76 W. In case 2, MSP once again offers the greatest possible maximum power 558.027 W, whereas the other configurations yield the highest possible maximum power 1112.2 W. For case 3, SP, BL, HC, and TCT offer the maximum power that is greatest 675.55 W, whereas MSP delivers the maximum power that is lowest 574.769 W. For case 4, the maximum power for SP, TCT, BL, HC, and MSP is (526.16, 558.03, 536.402, 536.4, 482.626) W. With these values, the TCT configuration offers the highest level of performance. For case 5, TCT and MSP show the greatest maximum power 675.55 W, whereas SP, BL, and HC deliver the lowest maximum power 574.77 W. Also, all possible PV array topologies concerning the shading loss, mismatch loss, and FF have been examined. Results indicate that all possible configurations result in the same shading loss for each scenario. The mismatch loss and FF were reduced for all three partial shading cases in which the MSP configuration excelled, which means that the PV array arrangement significantly affects the efficiency of the PV array. The effectiveness of a PV array is also influenced by factors such as the amount of available sunlight, the kind of shading present, and the incidence of such occurrences.

The results show that the proposed method in this research has a significant impact on improving the effectiveness of the PV system in even row, uneven row and diagonal shading cases, which means the greatest benefit from the PV system is if it is connected as MSP configuration. One of the obstacles that accompany MSP configuration is the interference that may occur between the wires connecting the solar modules.

REFERENCES

[1] L. F. L. Villa, D. Picault, B. Raison, S. Bacha, and A. Labonne, "Maximizing the power output of partially shaded photovoltaic plants through optimization of the interconnections among its modules," *IEEE Journal of Photovoltaics*, vol. 2, no. 2, pp. 154–163, Apr. 2012, doi: 10.1109/JPHOTOV.2012.2185040.

[2] S. Rezazadeh, A. Moradzadeh, S. M. Hashemzadeh, K. Pourhossein, B. Mohammadi-Ivatloo, and S. H. Hosseini, "A novel prime numbers-based PV array reconfiguration solution to produce maximum energy under partial shade conditions," *Sustainable Energy Technologies and Assessments*, vol. 47, p. 101498, Oct. 2021, doi: 10.1016/j.seta.2021.101498.

[3] K. A. Khudhur, N. M. A. Samad, and G. T. Hasan, "Investigate the maximum power point of photovoltaic system at different environmental conditions," *International Journal of Electrical and Computer Engineering*, vol. 13, no. 1, pp. 39–45, Feb. 2023, doi: 10.11591/ijece.v13i1.pp39-45.

[4] R. M. R. N. A. AL-Fakhry, "The effect of Co2 CH N2O Gases mission by using nueral network," *Al-Kitab Journal for Pure Sciences*, vol. 5, no. 2, pp. 41–54, 2021, doi: https://doi.org/10.32441/kjps.05.02.p4.

[5] A. Haines, G. Alleyne, I. Kickbusch, and C. Dora, "From the Earth Summit to Rio+20: Integration of health and sustainable development," *The Lancet*, vol. 379, no. 9832, pp. 2189–2197, Jun. 2012, doi: 10.1016/S0140-6736(12)60779-X.

[6] R. B. W. A. M. Ibrahim and R. R. Ibraheem, "Energy _Saving in_Batteries Using the Photovoltaic," *Al-Kitab Journal for Pure Science*, vol. 4, no. 1, 2020, doi: https://isnra.net/index.php/kjps/article/view/575.

[7] M. Saadsaoud, H. A. Abbassi, S. Kermiche, and M. Ouada, "Study of partial shading effects on photovoltaic arrays with comprehensive simulator for global MPPT control," *International Journal of Renewable Energy Research*, vol. 6, no. 2, pp. 413–420, 2016, doi: 10.20508/ijrer.v6i2.3426.g6801.

[8] O. Bingöl and B. Özkaya, "Analysis and comparison of different PV array configurations under partial shading conditions," *Solar Energy*, vol. 160, pp. 336–343, Jan. 2018, doi: 10.1016/j.solener.2017.12.004.

[9] J. C. Teo, R. H. G. Tan, V. H. Mok, V. K. Ramachandaramurthy, and C. Tan, "Impact of partial shading on the P-V characteristics and the maximum power of a photovoltaic string," *Energies*, vol. 11, no. 7, p. 1860, Jul. 2018, doi: 10.3390/en11071860.

[10] P. Raheem, "Performance of PV panel under shaded condition," *NTU Journal of Renewable Energy*, vol. 1, no. 1, pp. 22–29, 2021, doi: 10.56286/ntujre.v1i1.25.

[11] N. Hashim, N. F. N. Ismail, D. Johari, I. Musirin, and A. A. Rahman, "Optimal population size of particle swarm optimization for photovoltaic systems under partial shading condition," *International Journal of Electrical and Computer Engineering*, vol. 12, no. 5, pp. 4599–4613, Oct. 2022, doi: 10.11591/ijece.v12i5.pp4599-4613.

[12] A. Bernardini, A. Sarti, P. Maffezzoni, and L. Daniel, "Wave digital-based variability analysis of electrical mismatch in photovoltaic arrays," in *2018 IEEE International Symposium on Circuits and Systems (ISCAS)*, May 2018, pp. 1–5, doi: 10.1109/ISCAS.2018.8351026.

[13] S. R. Pendem and S. Mikkili, "Modeling , simulation , and performance analysis of PV array configurations (series , series-parallel, bridge-linked , and honey-comb) to harvest maximum power under various partial shading conditions," *International Journal of Green Energy*, vol. 00, no. 00, pp. 1–18, 2018, doi: 10.1080/15435075.2018.1529577.

[14] B. Yu and Y. Jung, "Performance analysis of a residential photovoltaic string under partial shading," *International Journal of Electrical and Computer Engineering*, vol. 13, no. 1, pp. 85–93, Feb. 2023, doi: 10.11591/ijece.v13i1.pp85-93.

[15] S. Pareek and R. Dahiya, "Output power maximization of partially shaded 4*4 PV field by altering its topology," *Energy Procedia*, vol. 54, pp. 116–126, 2014, doi: 10.1016/j.egypro.2014.07.254.

[16] H. Rezk, A. Fathy, and A. Y. Abdelaziz, "A comparison of different global MPPT techniques based on meta-heuristic algorithms for photovoltaic system subjected to partial shading conditions," *Renewable and Sustainable Energy Reviews*, vol. 74, pp. 377–386, Jul. 2017, doi: 10.1016/j.rser.2017.02.051.

[17] N. AJ. Khaleel and A. L. Mahmood, "Solar photovoltaic array reconfiguration for reducing partial shading effect," *Asian Journal of Convergence in Technology*, vol. 7, no. 2, pp. 114–120, Aug. 2021, doi: 10.33130/ajct.2021v07i02.022.

[18] A. Calcabrini, R. Weegink, P. Manganiello, M. Zeman, and O. Isabella, "Simulation study of the electrical yield of various PV module topologies in partially shaded urban scenarios," *Solar Energy*, vol. 225, pp. 726–733, Sep. 2021, doi: 10.1016/j.solener.2021.07.061.

[19] H. Patel and V. Agarwal, "MATLAB-based modeling to study the effects of partial shading on PV array characteristics," *IEEE Transactions on Energy Conversion*, vol. 23, no. 1, pp. 302–310, Mar. 2008, doi: 10.1109/TEC.2007.914308.

[20] F. Belhachat and C. Larbes, "Modeling, analysis and comparison of solar photovoltaic array configurations under partial shading conditions," *Solar Energy*, vol. 120, pp. 399–418, Oct. 2015, doi: 10.1016/j.solener.2015.07.039.

[21] M. Elyaqouti, D. Izbaim, and L. Bouhouch, "Study of the energy performance of different PV arrays configurations under partial shading," *E3S Web of Conferences*, vol. 229, p. 01044, Jan. 2021, doi: 10.1051/e3sconf/202122901044.

[22] S. Sajwan, M. K. Singh, and S. Urooj, "Physical relocation of PV panel for optimization of power under PSC in PV array," in *2018 IEEMA Engineer Infinite Conference, eTechNxT 2018*, Mar. 2018, pp. 1–6, doi: 10.1109/ETECHNXT.2018.8385322.

[23] D. Picault, B. Raison, S. Bacha, J. Aguilera, and J. De La Casa, "Changing photovoltaic array interconnections to reduce mismatch losses: A case study," in *2010 9th Conference on Environment and Electrical Engineering, EEEIC 2010*, 2010, pp. 37–40, doi: 10.1109/EEEIC.2010.5490027.

[24] G. Madhusudanan, N. Rakesh, S. S. Kumar, and S. S. Mary, "Solar photovoltaic array reconfiguration using Magic Su-Do-Ku algorithm for maximum power production under partial shading conditions," *International Journal of Ambient Energy*, vol. 43, no. 1, pp. 1204–1215, Dec. 2022, doi: 10.1080/01430750.2019.1691654.

[25] G. S. Krishna and T. Moger, "Improved SuDoKu reconfiguration technique for total-cross-tied PV array to enhance maximum power under partial shading conditions," *Renewable and Sustainable Energy Reviews*, vol. 109, pp. 333–348, Jul. 2019, doi: 10.1016/j.rser.2019.04.037.

[26] A. Djalab, N. Bessous, M. M. Rezaoui, and I. Merzouk, "study of the effects of partial shading on PV array," in *Proceedings - International Conference on Communications and Electrical Engineering, ICCEE 2018*, Dec. 2019, pp. 1–5, doi: 10.1109/CCEE.2018.8634512.

[27] R. Pachauri, R. Singh, A. Gehlot, R. Samakaria, and S. Choudhury, "Experimental analysis to extract maximum power from PV array reconfiguration under partial shading conditions," *Engineering Science and Technology, an International Journal*, vol. 22, no. 1, pp. 109–130, Feb. 2019, doi: 10.1016/j.jestch.2017.11.013.

BIOGRAPHIES OF AUTHORS

Parween R. Kareem obtained her bachelor's degree from Tikrit University, College of Engineering, Iraq in 2007, and her master's degree in electrical power engineering from the University of Mosul, College of Engineering, Iraq in 2008 and 2010. She is currently working as a teacher in the Department of Electrical Technologies at Hawija Technical Institute at Northern Technical University and head of the department of electrical technologies. Her research interests include renewable energy, power quality, high-quality utility interface, power electronics, power generation, and power grids. She can be contacted by e-mail: preween_hwj@ntu.edu.iq.

Algburi Sameer holds Ph.D. in electrical engineering. He has been a professor at Al-Kitab University since 2015. Head of research and study center at Victoria University, London. Member of the editorial board of several European journals, including sustainable resources management journal at Lund University (https://srwj.se/Boards) and the European Scientific Journal by European Scientific Institute ESI (https://eujournal.org/index.php/esj/announcement), and managing editor of Al-Kitab Journal for Pure Sciences (https://www.iasj.net/iasj/journal/328/jEditorial). Iraq's representative in the climate technology center and network program in Denmark CTCN of the United Nations UNEDO (https://www.ctc-n.org/network/network-members/al-kitab-university). He can be contacted at email: sameer.algburi@uoalkitab.edu.iq.

Husniyah Jasim received the B.Sc. and M.Sc. degrees in electrical engineering from Mosul University, Mosul, Iraq, in 1997 and 2020, respectively. She is currently the Head of the Department of Electronic Technologies at Al-Hawija Technical Institute, Northern Technical University. She can be contacted at email: husniyah_hwj@ntu.edu.iq.

Fattah H. Hasan received the B.Sc. and M.Sc. degrees in electrical engineering from Tikrit University, Tikrit, Iraq, in 2008 and 2013, respectively. he is currently a lecturer in the department of mechanical technologies at Al-Hawija Technical Institute, Northern Technical University. He can be contacted at email: fatah_hwj@ntu.edu.iq.